Advanced Steel Construction – Vol. 18 No. 3 (2022) 687–698
DOI:10.18057/IJASC.2022.18.3.6

SEGMENTED ASSEMBLY CONSTRUCTION FORMING METHOD WITHOUT BRACKETS OF SPATIAL CABLE-TRUSS STRUCTURE WITHOUT INNER RING CABLES

Jian Lu *, Su-Duo Xue, Xiong-Yan Li and Majid Dezhkam

College of Civil and Architecture Engineering, Beijing University of Technology, 100 Ping Le Yuan, Chaoyang District, Beijing 100124, China

** (Corresponding author: E-mail: lujian2020@126.com)*

ABSTRACT

Spatial cable-truss structure without inner ring cables (SCSWIRC) is a new cable-truss tension structure (CTTS), the features of which are composed of a series of planar cable-truss frames interwoven with each other. Its anti-collapse capacity is better, but its construction forming is complex. The reasons are that the strut's number and length will be enlarged with the span increase. Serious collision and winding of struts occur during construction due to SCSWIRC formed by a series of planar cable-truss frames interwoven with each other, which cause many difficulties in construction. According to the complex problem of construction forming, the segmented assembly construction forming method without brackets is proposed for SCSWIRC, and the basic idea of the proposed method is elaborated in detail. The SCSWIRC's experimental model with a 6m is designed, and numerical simulation and experimental research were carried out on the experimental model. The experimental results show that the error range of the internal forces of cables and struts is 6.99%~11.58%, and displacement errors of node 1 and node 2 are 3.27mm and 3.81mm, respectively verifies the feasibility and correctness of the proposed method. Then the static and dynamic experiment is carried out based on the final formed model. The static and dynamic experiment verifies the feasibility of the final formed model, which further shows the rationality and correctness of the segmented assembly construction forming method without brackets.

ARTICLE HISTORY

Received: 17 June 2021
Revised: 16 January 2022
Accepted: 31 January 2022

KEYWORDS

Spatial cable-truss structure without inner ring cables (SCSWIRC);
Segmented assembly without brackets;
Model design;
Construction forming;
Static and dynamic experiment

1. Introduction

At present, tensegrity structures are a research field that many scholars pay attention. More and more designers favor tensegrity structures because those kinds of structures have many good points, like little self-weight, beautiful appearance, strong spanning ability, and short construction period [1-3]. Meanwhile, cable-truss tension structures (CTTS) are one of the most typical structural forms of tensegrity structures. CTTS refers to the integral tension structure formed by the same kind of planar cable-truss frames according to certain layout principles. This kind of structure's common point is that the integral structure can be divided into planar cable-truss frames. Planar cable-truss frames share the same characteristics: lightweight, high stiffness, strong spanning ability, and simple construction. Now, CTTS mainly includes spoke cable-truss structures [4-5] shown in Fig. 1(a) and spatial cable-truss structures without inner ring cables shown in Fig. 1(b) [2-3,6]. The cable dome structure is a special CTTS [7,8] shown in Fig. 1(c).

Cable dome structure and spoke cable-truss structure have many practical projects domestic and overseas. There is an Olympics stadium in Seoul (1988) [9], the Florida Suncoast Dome in ST. Petersburg (1988) [10], the oval plan Levy form of cable dome for the Olympics in Georgia (1996) [11] in overseas. There is the National Fitness center in Ejin Horo Banner, Inner Mongolia (2012) [12], the Stadium of Tianjin University (2017) in domestic, and so on. For spoke cable-dome structures, there are Naka Stadium (1993), Kuala Lumpur Stadium (1998) [13], Busan Stadium (2001) [14] overseas. There are Shenzhen Bao'an Stadium (2001) [15], Yueqing Stadium (2013) [16], Zaozhuang Stadium (2017) in domestic. However, spatial cable-truss structure without inner ring cables is still in the theoretical and experimental research stage, and there are no practical projects domestic and overseas.

Through the research on SCSWIRC, it can be known that SCSWIRC is a novel CTTS, the features of which are composed of a series of planar cable-truss frames interwoven with each other [2-3,6]. It evolves from a spoke cable-truss structure with strong anti-collapse capacity because it has multiple load transfer paths [17]. Through the research on SCSWIRC, it can be known that although its anti-collapse capacity is excellent, its construction forming is more complicated. The reasons are that the strut's number and length will be enlarged with the span increase. Serious collision and winding of struts occur during construction due to SCSWIRC formed by a series of planar cable-truss frames interwoven with each other, which cause many difficulties in construction. If the strut's length is too long can be solved, the strut's collision and will be avoided during construction, which is beneficial to the structural application in projects. At present, SCSWIRC lacks the results related to construction forming. In contrast, construction forming is a significant problem faced by SCSWIRC, so it is necessary to carry out research related to its construction forming.

By studying construction forming's data, it can be known that the construction forming can be divided into two methods: construction forming method without brackets and construction forming method with brackets. The two methods have their advantages and disadvantages. The main difference is that the construction forming method without brackets avoids high-altitude operations and avoids using bed-jig, but it needs longer tooling cables; The construction forming method with brackets needs to use bed-jig to build a construction platform, which reduces the length of tooling cables but increases the project costs due to using bed-jig.

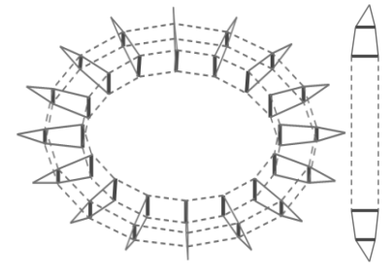

(a) Spoke cable-truss structure

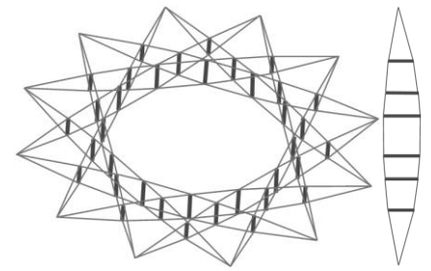

(b) Spatial cable-truss structure without inner ring cables

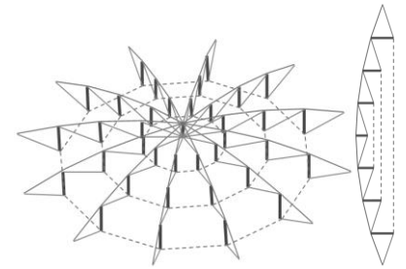

(c) Cable dome structure

Fig. 1 Three types of cable-truss tension structures

In order to solve the complicated problem of SCSWIRC's construction forming, the segmented assembly construction forming method without brackets is proposed based on the above discussions. The paper first elaborates on the segmented assembly construction forming without brackets. Then the SCSWIRC's experimental model with a 6m is designed. Moreover, the feasibility of the proposed method is verified by using numerical simulation and experimental research. Meanwhile, the final formed model is verified using the static and dynamic trials. Finally, the conclusions are given in the paper.

2. Segmented assembly construction forming method without brackets' basic idea

SCSWIRC is a new type of tensegrity structure. The topological relationship and structural features are different from the previous tensegrity structures, so its construction forming cannot wholly adopt the previous construction forming methods. The segmented assembly construction forming method without brackets is proposed in the paper based on the structural characteristics of SCSWIRC. The solved flow of the new construction forming method is shown in Fig. 2a.

The basic idea of the new method: the main cable system structure in Fig. 2a can be divided into three parts: upper single-layer crossed cable net formed by upper chord cables in Fig. 2b, lower single-layer crossed cable net formed by lower chord cables in Fig. 2b, and struts connecting upper and lower single-layer crossed cable nets in Fig. 2c. Then use tooling cables to stretch the upper single-layer crossed cable net to a certain height. Moreover, assemble the segmented struts in Fig. 2c. After the last section of struts is raised to a certain height, the lower single-layer crossed cable net is assembled, and cable nets and struts are fixed with particular cable-strut joints. Finally, the assembled main cable system structure is lifted to the design configuration using tooling cables, which are connected and fixed with ring beams. The schematic diagram of the construction forming process for SCSWIRC is shown in Fig. 2d.

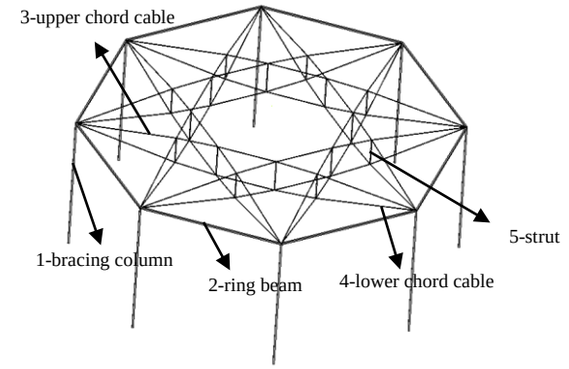

(a) Spatial cable-truss structure without inner ring cables

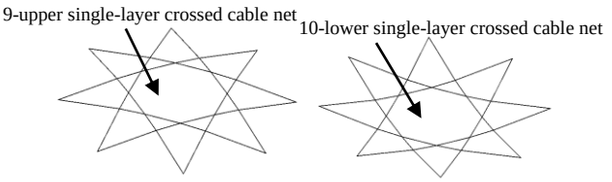

(b) Upper and lower single-layer crossed cable net

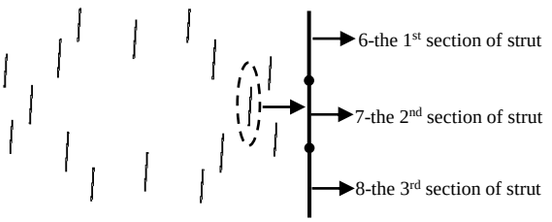

(c) Schematic diagram of segmented strut

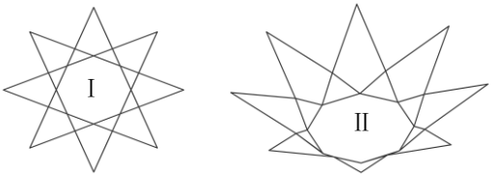

Ⅰ Segment upper single-layer crossed cable net on the ground
Ⅱ Lift upper single-layer crossed cable net to a certain height

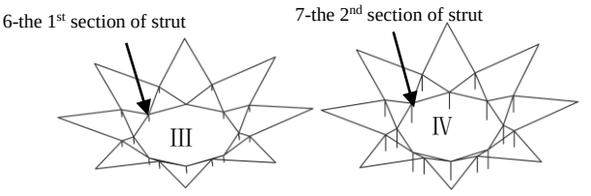

Ⅲ Segment the 1st section of strut Ⅳ Segment the 2nd section of strut

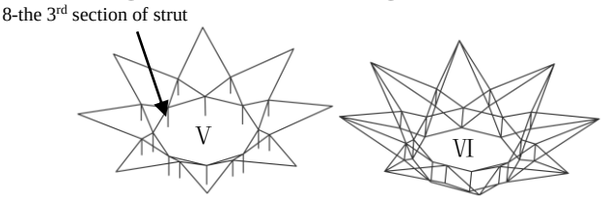

Ⅴ Segment the 3rd section of strut Ⅵ Segment lower single-layer crossed cable net on the ground

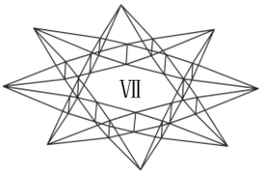

Ⅶ Stretch main cable system structure to design configuration

(d) Steps of construction forming based on proposed method

Fig. 2 Relative diagrams of segmented assembly construction forming method without brackets

According to Fig. 2, the steps of the segmented assembly construction forming method without brackets are as follows:

The 1st step: Install bracing column 1 and ring beam 2 according to the construction scheme. Then check whether the position of bracing column 1 is correct or not and whether the ring beam 2 is installed to the design height or not;

The 2nd step: Assemble upper single-layer crossed cable net 9 formed by upper chord cables according to non-stress cable length in the center of a construction site, and fix and clamp the joints among crossed cable net.

The 3rd step: Install the tooling cables of upper single-layer crossed cable net and then connect tooling cables and lifting equipment;

The 4th step: Use synchronous lifting equipment like hydraulic jacks to slowly lift tooling cables of upper single-layer crossed cable net 9 to a certain height (provide a construction platform for workers to facilitate following construction process);

The 5th step: At this time, install the first section 6 of strut using the height difference between upper single-layer crossed cable net and the ground according to construction scheme and then connect it with upper single-layer crossed cable net 9;

The 6th step: Continue lifting the upper single-layer crossed cable net 9 to a certain height, and then segment the 2nd section of strut 7. Flanges are used to connect the 2nd section of strut 7, which is bolted or welded;

The 7th step: Repeat the 4th~5th steps until all segmented struts are assembled;

The 8th step: Assemble lower single-layer crossed cable net 10 formed by lower chord cables according to non-stress cable length in the center of the construction site, and then fix and clamp the joints among crossed cable net;

The 9th step: Install the tooling cables of lower single-layer crossed cable net 10 and connect it with lifting equipment together;

The 10th step: Connect lower single-layer crossed cable net 10 with the last section of strut 8 together. At this time, the whole structure's relaxed state is formed by an upper single-layer crossed cable net with stresses and a lower single-layer crossed cable net without stresses.

The 11th step: Stretch tooling cables of the segmented central cable system to the design configuration, and then connect the ends of the upper and lower single-layer crossed cable net with a ring beam. At this time, the whole process of construction forming is completed.

The method is considered from the perspectives of actual construction (the spans of practical projects are generally greater than 200m), which avoids collision and winding among struts and crossed cable nets due to a large number of struts and too long length of struts and avoids high-altitude operations and improves construction efficiency and guarantees construction quality. The proposed method provides a practical and feasible way for SCSWIRC and promotes the application of SCSWIRC in projects to a certain extent. Meanwhile, the segmented assembly construction forming method without brackets can also be applied to other tensegrity structures with rigid struts.

3. Model design

In order to verify the feasibility and correctness of the segmented assembly construction method without brackets, a trial model with a diameter of 6m is designed for SCSWIRC. The trial model design includes the main cable system structure, ring beam, bracing column, cable-strut joint, cable-beam joint, and strut connector.

3.1. Material property experiment

Considering the unknown mechanical properties of cable and strut, four groups of cable and strut test-pieces were selected from the same batch of materials, shown in Fig. 3. The cable and strut mechanical properties are calibrated at the Strength Testing Institute of Beijing University of Technology. The mean values of trial results are used as the final trial values. The material properties of cable and strut obtained through material property experiment are shown in Table 1.

3.2. Design of main cable system structure

The main cable system structure comprises the upper and lower single-layer crossed cable net and strut, which is the central force of SCSWIRC. Its main cable system structure can be seen as composed of N planar cable-truss frames, and N is equal to 10 in the paper's trial model shown in Fig. 4a. Both

Fig. 3 Test-pieces of cable and strut

Table 1
Material properties of cable and strut

Element Type	Size	Area /mm^2	Elastic modulus/MPa	Broken force/kN
Cable	Φ6	21.487	1.21*10^5	36
Strut	P20*3	141.300	2.05*10^5	52.02

planar cable truss frame's upper and lower chord cables conform to parabola's shape like Eq. (1). According to Ref. [18], it can be known that the ranges of the optimal rise-span ratio of upper and lower chord cables are 1/25~1/20 and 1/20~1/15, respectively. So, the rise-span ratios of upper and lower chord cables are selected as f_u=1/24 and f_b=1/16, respectively. All Eq. (1) parameters can be solved according to f_u, f_b, N, and d, so A_1=-0.091778, B_1=0.075665, A_2=0.137668 B_2=-0.113497. The program of solving nodal coordinates is compiled based on the layout relationship of cable-truss frames and Fortran Language. The solved nodal coordinates are shown in Table 2. The geometry model formed by all nodal coordinates is shown in Fig. 4b. The feasible self-stress mode of the geometry model can be solved using Ref. [19], and the results are shown in Table 3. The integral finite element model can be obtained according to the feasible self-stress mode in Table 3, the finite element model shown in Fig. 4c.

$$\begin{cases} y_1 = A_1 x_1^{\ 2} + B_1, A_1 < 0 \\ y_2 = A_2 x_2^{\ 2} + B_2, A_2 > 0 \end{cases} \tag{1}$$

3.3. Design of ring beam and bracing column

The ring beam is made of H-shaped steel, and its size is H200×200×12×12. The bracing column is made of circular

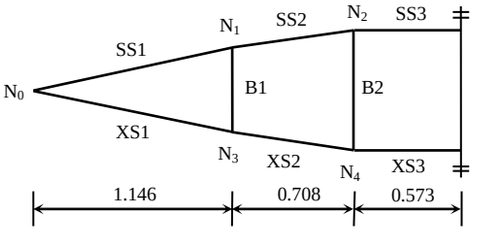

(a) Planar cable-truss frame Unit: m

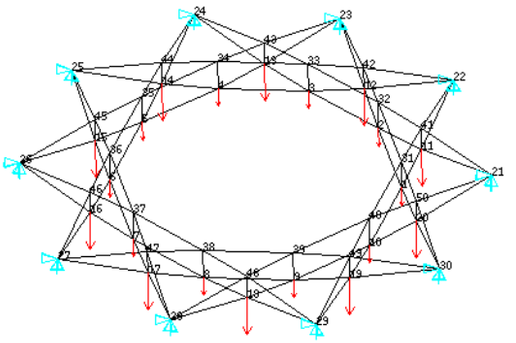

(b) Geometry model and nodal number

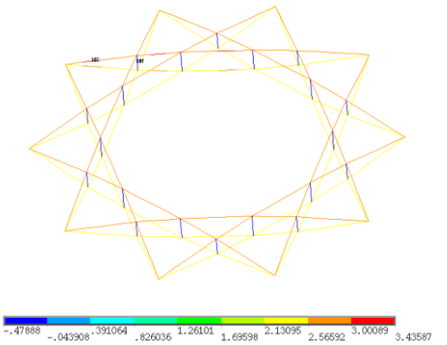

(c) Finite element model Unit: kN

Fig. 4 Main cable system structure of geometry model

Table 2
Nodal coordinates of geometry model

Nodal number	*x*/*m*	*y*/*m*	*z*/*m*	Nodal number	*x*/*m*	*y*/*m*	*z*/*m*	Nodal number	*x*/*m*	*y*/*m*	*z*/*m*	Nodal number	*x*/*m*	*y*/*m*	*z*/*m*	Nodal number	*x*/*m*	*y*/*m*	*z*/*m*
1	3.000	0.000		11	2.073	0.674		21	1.854	0.000		31	2.073	0.674		41	1.854	0.000	
2	2.427	1.763		12	1.281	1.763		22	1.500	1.090		32	1.281	1.763		42	1.500	1.090	
3	0.927	2.853		13	0.000	2.180		23	0.573	1.763		33	0.000	2.180		43	0.573	1.763	
4	-0.927	2.853		14	-1.281	1.763		24	-0.573	1.763		34	-1.281	1.763		44	-0.573	1.763	
5	-2.427	1.763	0.000	15	-2.073	0.674	0.159	25	-1.50	-1.090	0.208	35	-2.073	0.674	-0.195	45	-1.500	1.09	-0.255
6	-3.000	0.000		16	-2.073	-0.674		26	-1.854	0.000		36	-2.073	-0.674		46	-1.854	0.000	
7	-2.427	-1.763		17	-1.281	-1.763		27	-1.0500	-1.090		37	-1.281	-1.763		47	-1.500	-1.090	
8	-0.927	-2.853		18	0.000	-2.180		28	-0.573	-1.763		38	0.000	-2.180		48	-0.573	-1.763	
9	0.927	-2.853		19	1.281	-1.763		29	0.573	-1.763		39	1.281	-1.763		49	0.573	-1.763	
10	2.427	-1.763		20	2.073	-0.674		30	1.500	-1.090		40	2.073	-0.674		50	1.500	-1.090	

Table 3
Feasible self-stress mode of geometry model

Nodal number	Cable						Strut	
	SS1	SS2	SS3	XS1	XS2	XS3	B1	B2
Cable length/m	1.157	0.7104	1.146	1.163	0.7106	1.146	0.354	0.463
Non-stress cable length/m	1.153	0.7090	1.142	1.161	0.7094	1.144	–	–
internal force/kN	3.416	3.392	3.381	2.848	2.818	2.805	-0.476	-0.472

Steel tube of P89×5. The ring beam and bracing column are all Q235 steel, and the detailed diagram of the ring beam and bracing column are shown in Fig. 5.

3.4. Design of cable-strut joint

The design rules of cable-strut joints: (1) Try not to cut cables as much as possible so that the whole cable can pass through cable-strut joints. That is, cables are continuous and through; (2) Joints can significantly reflect structural characteristics;

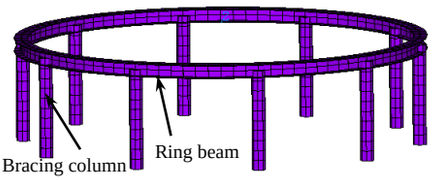

(a) Finite element model

(b) Solid model

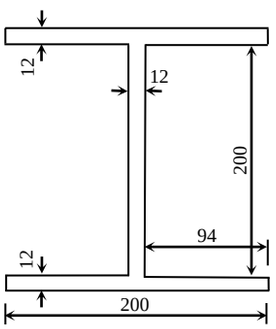

(c) Size of ring beam

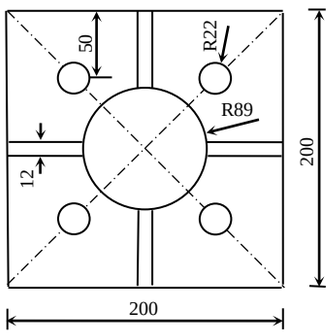

(d) Detailed diagram of column's top

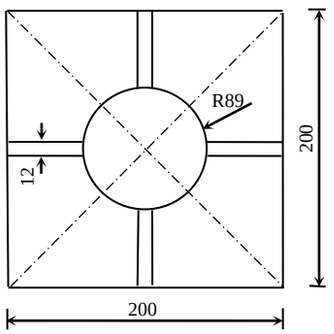

(e) Detailed diagram of column's foot

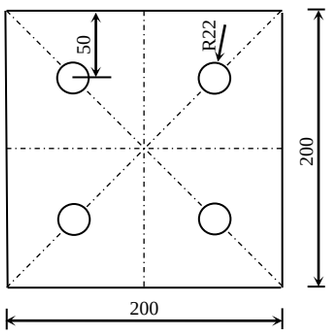

(f) Cover plate between ring beam

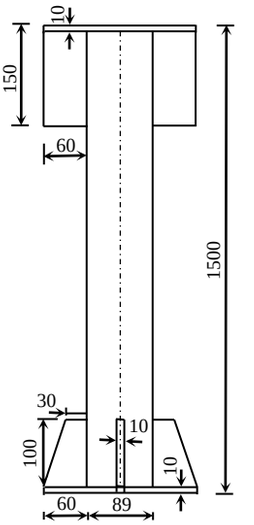

(g) Detailed diagram of bracing column

Fig. 5 Model and detailed diagram of ring beam and bracing column

(3) Joints should be as simple as possible, and the force transmission road is clear; (4) Joints can have a small amount of rotation so that joints can be fine-tuned to make cables pass through the strut's center after assembling the main cable system structure. According to the above four design rules, the detailed diagram of the cable-strut joint is shown in Fig. 6.

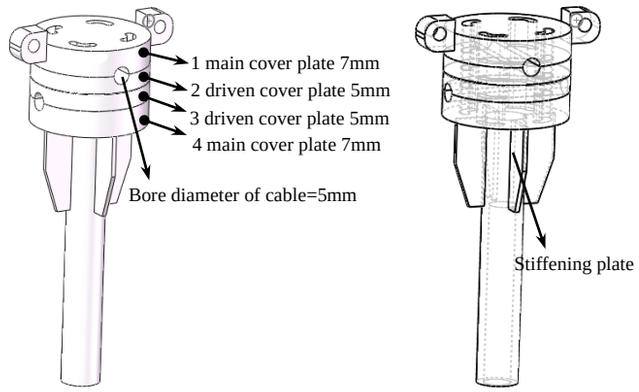

(a) Three-demission diagram of cable-strut joint

(b) Detailed diagram of cover plate

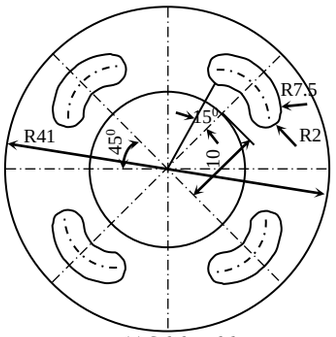

(c) Solid model

Fig. 6 Detailed diagram of cable-strut joint

3.5. Design of cable-beam joint

The design of the cable-beam joint should be based on the angle between every two cable-truss frames like nodes 21~30 in Fig. 4b. The cable-beam joint's correlation diagram is shown in Fig. 7.

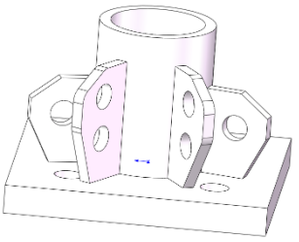

(a) Three-demission model

(b) Solid model

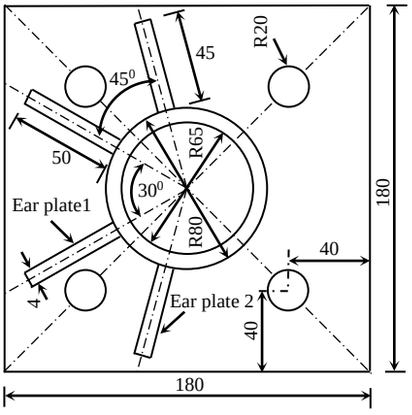

(c) Graphic diagram

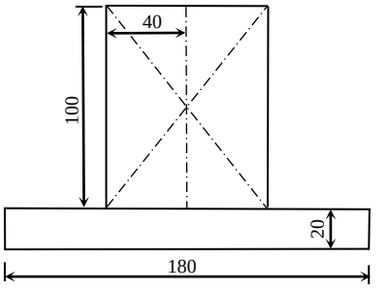

(d) Elevation diagram

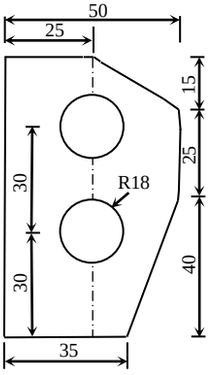

(e) Ear-plate 1

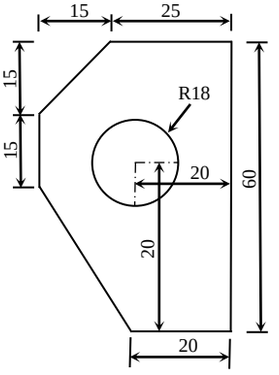

(f) Ear-plate 2

Fig. 7 Correlation diagram of cable-beam joint

3.6. Design of strut connector

It needs to divide struts into several sections in advance when using segmented assembly construction forming method without brackets. Flanges are used to connect the sections of struts, shown in Fig. 8.

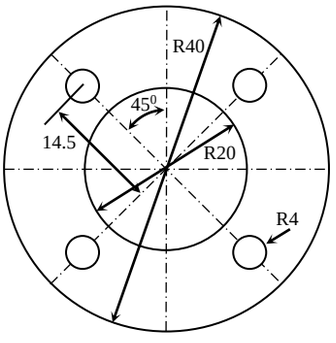

(a) Detailed diagram of flange

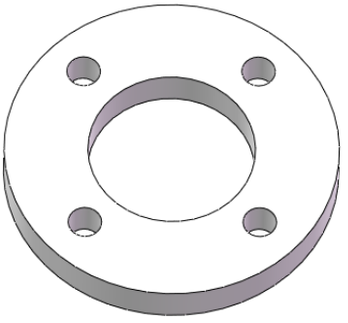

(b) Three-demission model of flange

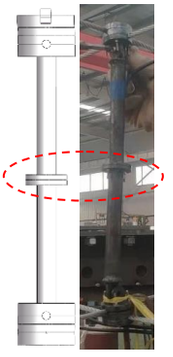

(c) solid model of strut B1

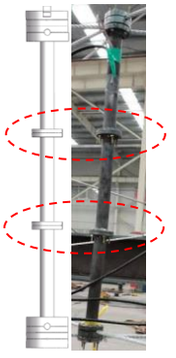

(d) solid model of strut B2

Fig. 8 Correlation diagram of strut connector

4. Construction forming trial based on segmented assembly construction forming method without brackets

4.1. The influence of ring beam and bracing column on main cable system structure

It can be known from Ref. [3] that ring beam and bracing column have some influence on SCSWIRC, so the influence should be considered during construction forming. The integral finite element model is shown in Fig. 9.

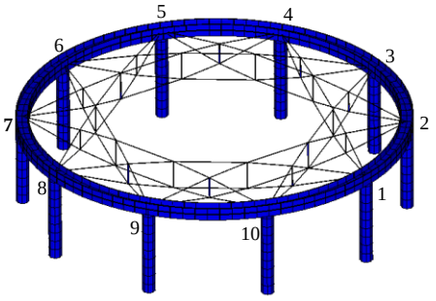

Fig. 9 Integral finite element model

4.2. Layout of monitoring points in trial

Cable-strut joints are node 1~10, shown in Fig. 9. The trial model can be divided into 10 planar cable-truss frames based on the number of cable-beam joints, including cable-truss frame 1-4, cable-truss frame 2-5, cable-truss frame 3-6, cable-truss frame 4-7, cable-truss frame 5-8, cable-truss frame 6-9, cable-truss frame 7-10, cable-truss frame 8-1, cable-truss frame 9-2, cable-truss frame 10-3. The internal forces of upper and lower chord cables and struts are monitored during construction. Meanwhile, the z-components of all nodal displacements for these two cable-truss frames are monitored in crucial steps of construction forming. Monitoring points of internal forces and displacements are shown in Fig. 10. Cable-truss frames 1-4 and cable-truss frames 6-9 are in symmetrical positions in Fig. 9.

During the experiment, strain gauges were used to monitor the change of cables and struts' internal forces, attached to pre-designed threaded sleeves shown in Fig. 10. All the strain gauges are connected to the static collection instrument JM3813 through the collection line, shown in Fig. 11a. Static collection instrument JM3813 collects the signal and transmits the signal to a computer. Finally, the signal is converted into strain by computer, and the internal force values of cables and struts can be obtained by further calculation. Level gauge and steel ruler are used to monitor nodal displacement of the cable-truss frame at critical positions, shown in Fig. 11b.

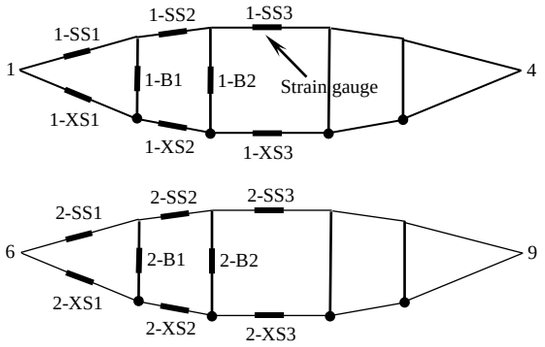

Fig. 10 The layout of monitoring points of internal forces and displacements

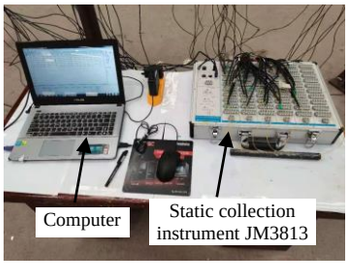

(a) Static collection instrument

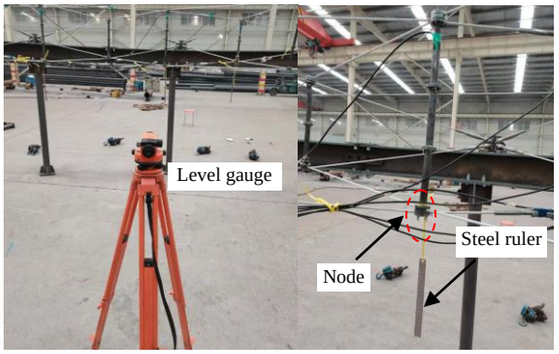

(b) Level gauge and steel ruler

Fig. 11 Static collection instrument JM3813, level gauge and steel ruler

4.3. Segmented assembly construction forming trial

The segmented assembly construction forming method is a new construction forming method that can solve the complex problem of construction forming for SCSWIRC in concept. However, it is still necessary to further verify the feasibility and effectiveness of the proposed method in experiment. The paper adopts the construction forming mode with the fixed-length cable. The non-stress cable length can be obtained based on the finite element model in Fig. 4b, shown in Table 3.

The "segment" for segmented assembly construction forming method without brackets refers to dividing struts into several sections in advance. Then the segmented struts are assembled section by section in construction. In experiment, strut B1 and B2 are divided in advance. The strut B1 is divided into two sections, including B11 and B12; the strut B2 is divided into three sections, B21, B22, and B23, as shown in Fig. 12. The construction forming process is divided into six key steps according to segmented assembly construction forming method characteristics without brackets.

The 1st step: Install the upper single-layer crossed cable net on the ground;

The 2nd step: Use tooling cables and synchronous lifting equipment to lift the upper single-layer crossed cable net to a certain height, and then assemble the 1st section of the strut on the ground. The 1st section of strut and upper single-layer crossed cables are fixed and clamped with cable-strut joints;

The 3rd step: Continue lifting the segmented parts to a certain height, and then assemble the 2nd section of a strut. Flanges connect the 1st section of strut and 2nd section of the strut;

The 4th step: Continue lifting the segmented parts to a certain height, and then assemble the 2nd section of the strut. The 2nd section of the strut and the 3rd section of strut are connected by flanges;

The 5th step: Continue lifting the segmented parts to a certain height, and then assemble a lower single-layer crossed cable net. The segmented parts and lower single-layer crossed cable net are fixed and clamped by cable-strut joints;

The 6th step: Use tooling cables and synchronous lifting equipment to lift the segmented main cable system structure to design configuration.

Strut B1 is divided into two sections, so its construction steps are steps 1~3 and steps 5~6. Strut B2 is divided into three sections, so its construction steps are steps 1~6. Due to adopting construction forming mode with the fixed-length cable, the configuration and cable forces generally conform to the design values after the main cable system structure is stretched to design configuration when the manufacturing errors of ring beam, cable, and strut are not considered. When cable forces and configuration do not meet design values, the length of the threaded sleeve of the cable's ends can be adjusted appropriately to compensate for the manufacturing and assembly process errors.

The methods of solving the convergence problem of construction forming based on ANSYS finite element software include: (1) Ref. [20] proposed the extensive temperature method to improve the convergence of construction simulation. (2) Ref. [21] proposed the added cables method to improve the convergence of construction simulation. (3) Ref. [22] proposed the inverse-construction and rigid displacement methods. The convergence problem of construction simulation was solved by the inverse-construction method and applying rigid displacement on nodes that are prone to rigid displacement. (4) Ref. [23] proposed the effective damping method that can improve the convergence of construction simulation by applying significant damping to structures to make the structure be in a viscoelastic liquid environment. (5) Ref. [24] proposed the added beam method to solve the convergence problem of construction simulation. (6) Ref. [25] proposed the nodal displacement hypothesis to improve the convergence of construction simulation. The paper solves the convergence problem of construction simulation of SCSWIRC based on Ref. [20] and Ref. [22].

Meanwhile, due to the SCSWIRC's construction forming from ground to the design configuration belonging to large displacement and deformation, the internal forces of cables and struts can be monitored in the whole construction, but the changes of nodal displacement are difficult to monitor. So, the experimental values of nodal displacement of cable-truss frame 1-4 and cable-truss frame 6-9 in Fig. 10 are only given when the length of tooling cables is 5cm, 4cm, 3cm, 2cm, 1cm and 0cm. That is, the construction process is divided into six key steps. The six key steps of construction simulation and construction forming trial are shown in Fig. 13.

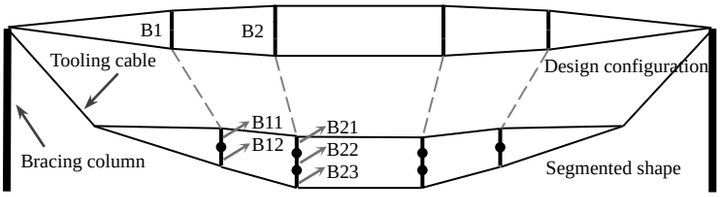

Fig. 12 Schematic diagram of strut's segments of single cable-truss frame

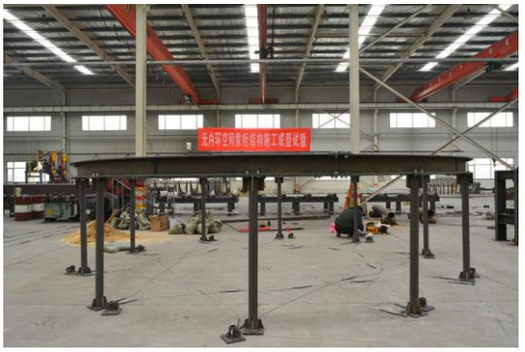

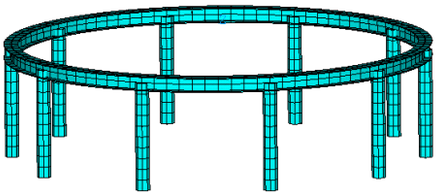

Start: Install ring beam and bracing column

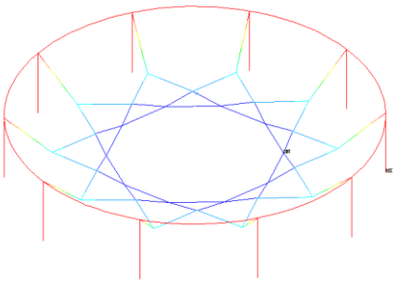

The 1st step: Assemble upper single-layer crossed cable net on the ground and install tooling cables

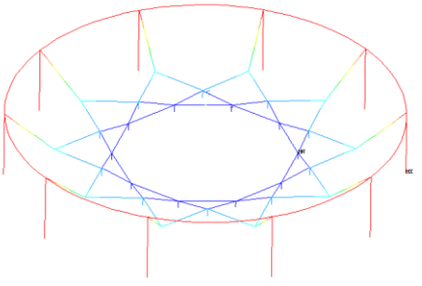

The 2nd step: Lift upper single-layer crossed cable net to a certain height and then assemble strut B11 and B21

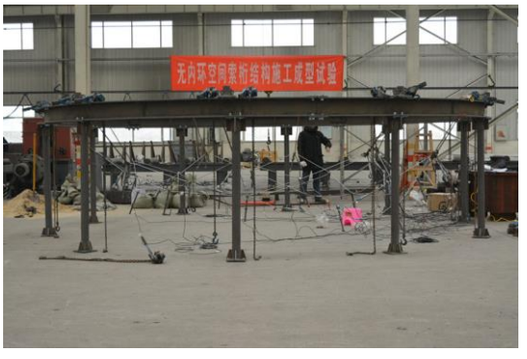

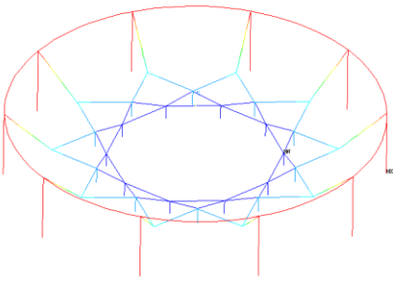

The 3rd step: Continue lifting the segmented parts to a certain height and then assemble B12 and B22

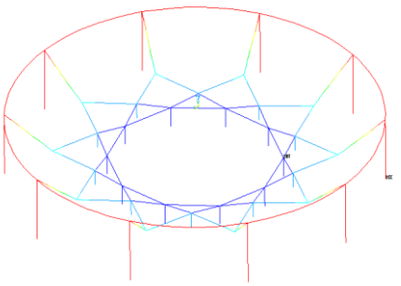

The 4th step: Continue lifting the segmented parts to a certain height and then assemble B23

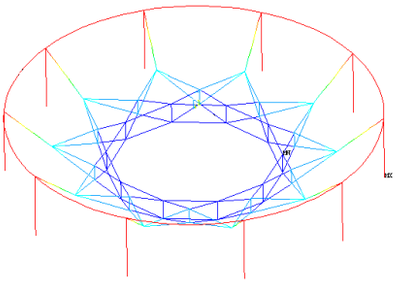

The 5th step: Continue lifting the segmented parts to a certain height, and then assemble a lower single-layer crossed cable net and connect it with the segmented parts

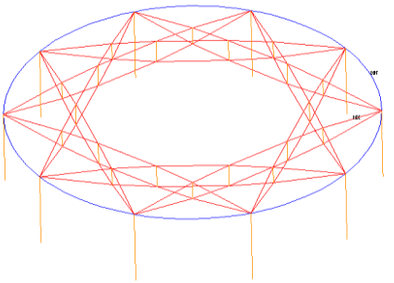

The 6th step: Continue lifting the segmented main cable system structure to design height and then dismantle tooling cables and connect it with ring beam together.

Fig. 13 The experimental process of segmented assemble construction forming method without brackets

In the experiment, the internal forces of cables and struts and nodal displacements for cable-truss frame 1-4 and cable-truss frame 6-9 are monitored. Cable-truss frame 1-4 and cable-truss frame 6-9 are in the symmetric position and the experimental datum is the same, so take cable-truss frame 1-4 as an example and give the detailed data in construction. The comparison results of simulation values and experimental values are shown in Table 4 and Fig. 14.

Table 4
Internal forces of cables and struts in the six key steps of construction

Nodal number	Key construction steps						Nodal number	Key construction steps					
	1th	2th	3th	4th	5th	6th		1th	2th	3th	4th	5th	6th
SS1- experimental value	–	0.0065	0.00649	0.00645	0.0064	3.654	XS1-experimental value	–	–	–	–	0.0218	3.137
SS1-simulation value	–	0.0055	0.00539	0.00565	0.0073	3.416	XS1-simulation value	–	–	–	–	0.0243	2.848
SS2- experimental value	–	0.0041	0.00413	0.0041	0.0041	3.673	XS2- experimental value	–	–	–	–	0.0211	3.048
SS2-simulation value	–	0.0055	0.0037	0.0057	0.0049	3.392	XS2-simulation value	–	–	–	–	0.0245	2.818
SS3- experimental value	–	0.00078	0.00079	0.00079	0.00080	3.732	XS3- experimental value	–	–	–	–	0.0238	3.103
SS3-simulation value	–	0.00063	0.00066	0.00084	0.00092	3.381	XS3-simulation value	–	–	–	–	0.0292	2.805
B1- experimental value	–	-0.0047	-0.0047	-0.0047	-0.0047	-0.522	B2- experimental value	–	0.0053	0.0053	0.0053	-0.0054	-0.508
B1-simulation value	–	-0.0085	-0.0078	-0.0059	-0.0063	-0.476	B2-simulation value	–	0.0036	0.0074	0.0085	-0.0056	-0.472

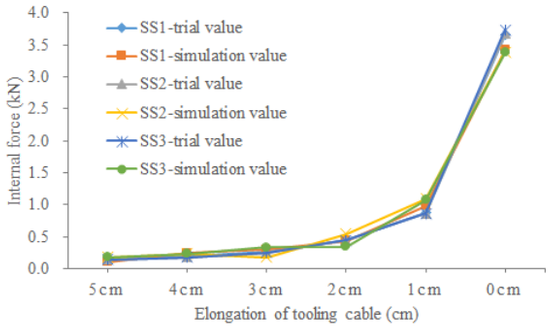

(a) Internal forces of upper chord cables

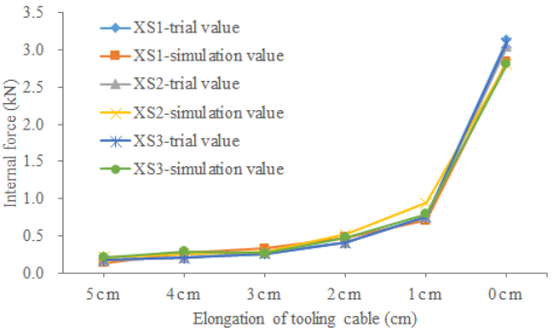

(b) Internal forces of lower chord cables

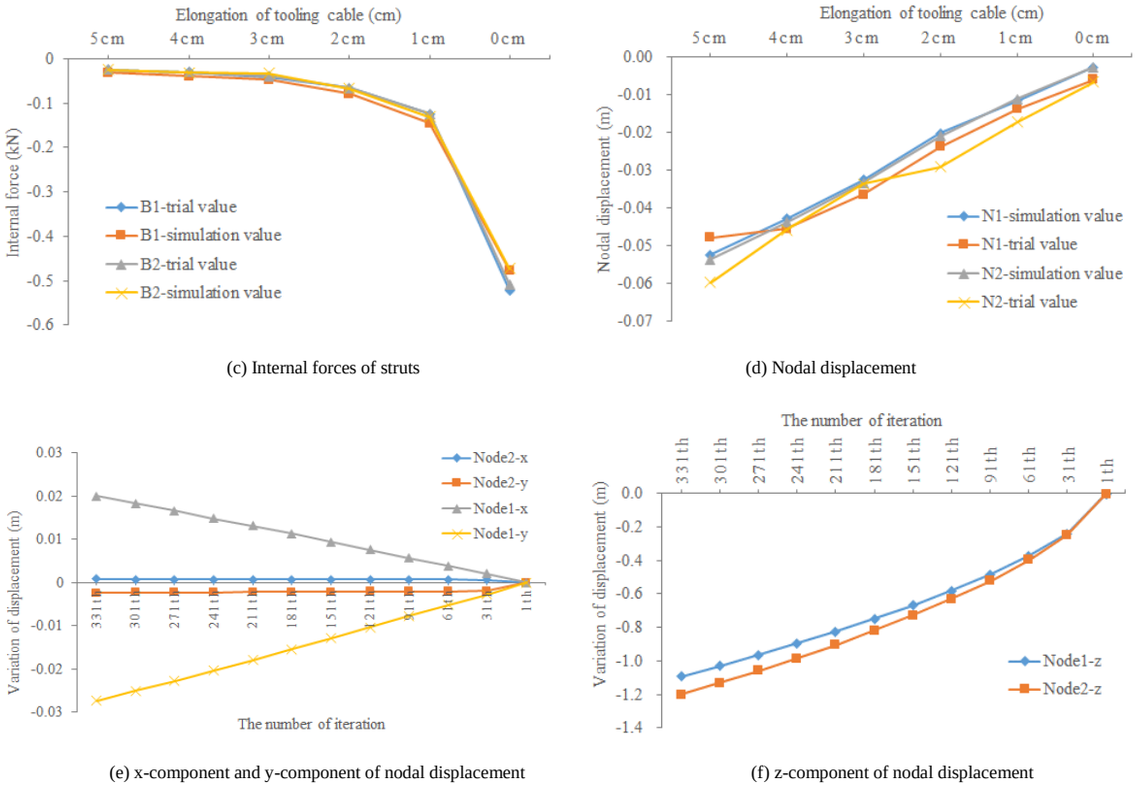

(c) Internal forces of struts

(d) Nodal displacement

(e) x-component and y-component of nodal displacement

(f) z-component of nodal displacement

Fig. 14 Change curves of internal forces of cables and struts and nodal displacement in experiment

In ANSYS finite element software, the inverse construction method can complete the construction simulation in Fig. 13 [22]. It can be seen from the experimental process that construction forming steps are simple and the operation is convenient, and the construction forming process is relatively smooth. The SCSWIRC's construction forming belongs to an extensive deformation process. At the same time, it can be seen from the construction forming process in Fig. 13 that the upper chord cables are in a relaxed state in the 1st step, so the values of the internal forces cannot be measured. The struts are not assembled in the 1st step, so their internal forces cannot be measured. The lower chord cables start to install in the 5th step, so their internal forces can be measured in the 5th step. It can be seen from Table 4 and Fig. 14(a)~(d) that experimental values and simulation values are identical. The internal forces of upper and lower chord cables increase with the decrease of the length of tooling cables. The main cable system structure is stretched to design configuration when the length of tooling cables is shortened to zero. Then the final formed model will conform to the design shape by cable's fine-tuning threaded sleeve several times. In the final formed state, the error range of upper chord cables' internal forces is 6.99%~10.2%; the error range of lower chord cables' internal forces is 8.20%~11.58%; the error range of struts' internal forces is 9.21%~11.31%.

The displacement errors of node 1 and node 2 are 3.27mm and 3.81mm, respectively. The errors are within the acceptable range. The main reasons for errors are the drift of strain gauge, the manufacturing and construction errors, and measuring instrument errors. Fig. 14(e)~(f) shows that the changing trend of displacement components of node 1 and node 2 in the *x*, *y*, *z* directions during the whole construction forming experiment. It can be seen from Fig. 14(e)~(f) that the x and y coordinate values change very little and linearly in construction. Nevertheless, the changes in the z-component are significant and nonlinear, so the total displacement of three components x, y, and z are also nonlinear, which is consistent with the nonlinear nature of large deformation in construction forming. So, it can be seen from the analysis results that the segmented assembly construction forming method without brackets can solve the difficulty of SCSWIRC's construction forming.

4.4. Further discussions

(1) There are lots of struts for SCSWIRC with a large span, and its length is long. When a segmented assembly construction forming method without brackets is used, struts will be divided into several sections. The segmented struts are connected with flanges, so many cable-strut joints and flanges will significantly increase workers' workload. While jumping layout or removed struts can simplify SCSWIRC [2]. Jumping layout means that a strut that needs to be removed is not modeled in design, and structural integrity is not damaged. Therefore, the grid-jumped layout differed from the broken cable and broken strut. The process of grid-jumped layout for SCSWIRC is shown in Fig. 15. The grid-jumped layout's positions should be symmetrical to ensure structural symmetry and integrity. The number of struts will decrease after grid-jumped layout, and the number of cable-strut joints and flanges will also decrease. So, jumping layout reduces project cost and worker's workload and saves time to a certain extent.

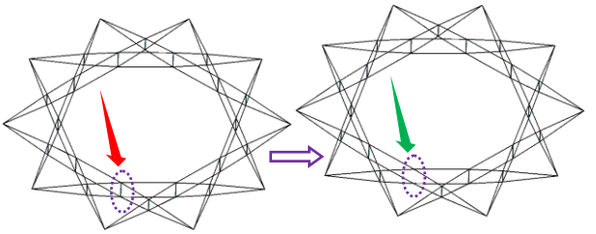

Fig. 15 Grid-Jumped layout's process of SCSWIRC

(2) When the segmented assembly construction forming method without brackets is used, struts will be divided into several sections, and flanges connect the segmented struts. If the segmented positions of all struts are the same as shown in Fig. 16a, a segmented surface will be generated at all segmented positions. The segmented surface is a weak part, which is unfavorable to SCSWIRC. The struts need to be staggered in segmented positions (shown in Fig. 16b). The segmented positions of all struts do not form segmented surfaces at a certain height, eliminating the safety hazards brought by segmented surfaces.

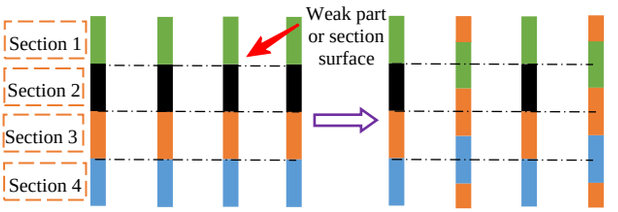

(a) Segmented positions of struts are the same (b) Segmented positions of struts are not same

Fig. 16 Schematic diagram of segmented position of struts

5. Static and dynamic experiment

5.1. Static experiment

In order to verify the static performance of the final formed model, the static loading experiment is carried out on the final formed model. Static loading experiment includes full-span loading experiment and half-span loading experiment, shown in Fig. 17. The formed experimental model's equivalent nodal load **F** can be obtained by solving equivalent nodal load in Ref. [2]. In Fig. 4a, the equivalent load of node 1 is F_1=0.429kN, the equivalent load of node 2 is F_2=0.361kN, that is, **F**=10*[F_1, F_2]. The static loading trial uses sandbags to load step by step. When the load is 0.8**F**, 0.9**F**, 1.0**F**, 1.1**F**, 1.2**F**, structural static response is investigated respectively.

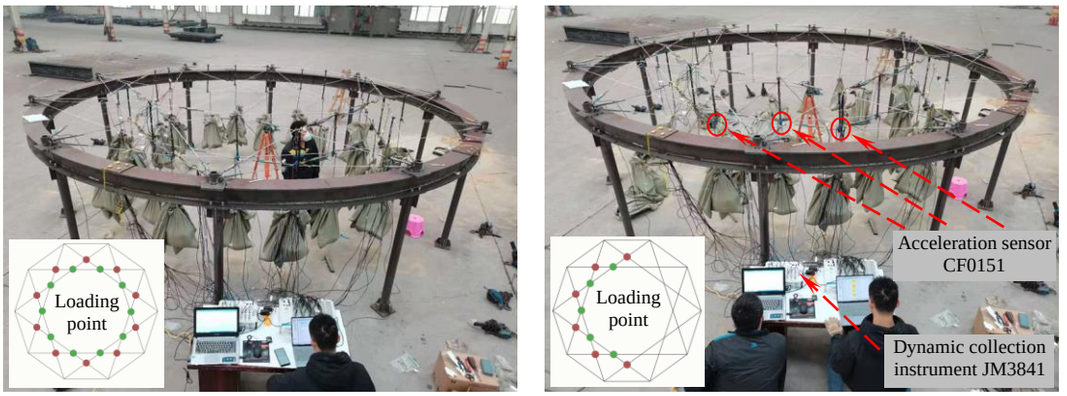

(a) Full-span laods (b) half-span loads

Fig. 17 Layout diagram of full-span loads and half-span loads

5.1.1. Under full-span loads

The responses of internal forces and displacements of the structure under full-span loads are shown in Fig. 18.

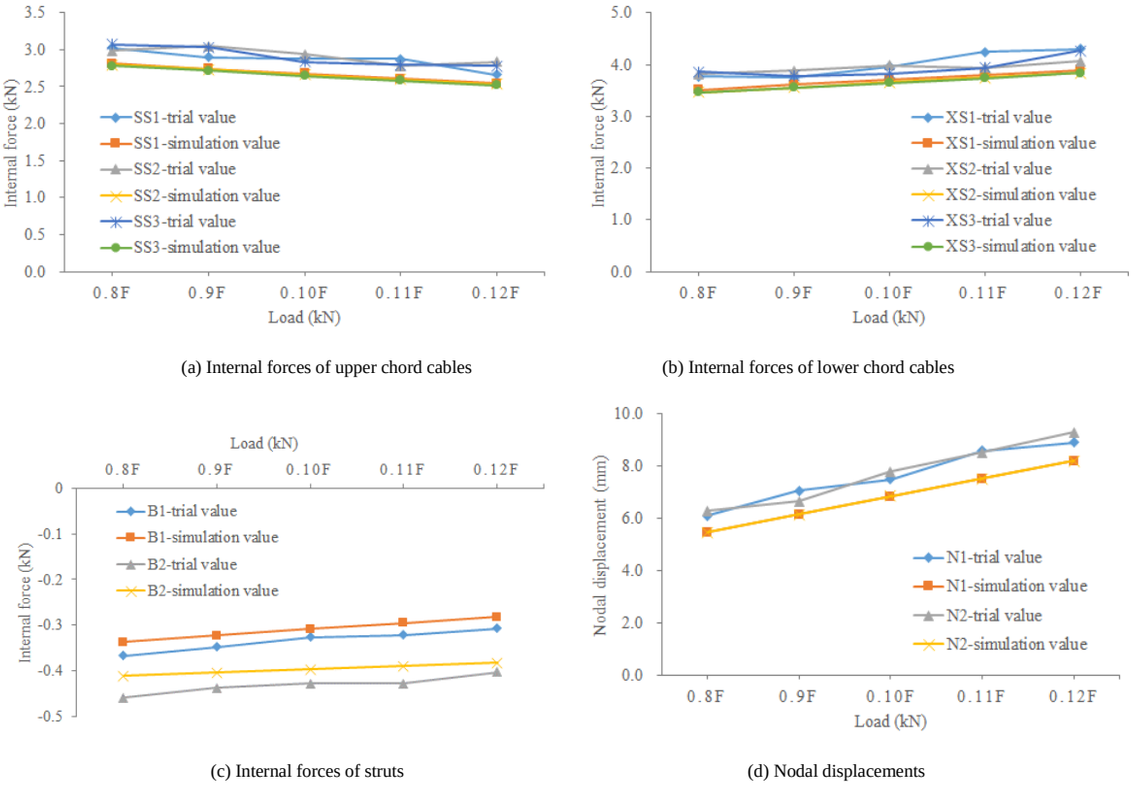

(a) Internal forces of upper chord cables (b) Internal forces of lower chord cables

(c) Internal forces of struts (d) Nodal displacements

Fig. 18 Internal forces of cable and strut and nodal displacements under full-span loads

It can be seen from Fig. 18 that the internal forces of cables and struts and nodal displacements linearly change under full-span loads, which shows that the final formed model has an excellent static performance. With the increase of loads, the internal forces of upper chord cables are decreasing; the internal forces of lower chord cables and struts are increasing; nodal displacements are increasing. The change laws of internal forces and cables and struts and nodal displacements conform to the mechanical characteristics of those kinds of structures. Under load 0.8**F**~1.2**F**, the maximum error of internal forces of upper chord cables SS1~SS3 is 11.61%; the maximum error of internal forces of lower chord cables XS1~XS3 is 10.16%; the maximum error of internal forces of struts B1~B2 is 10.43%; the maximum errors of displacement of nodes N_1 and N_2 are 10.86% and 12.89%, respectively. Technical Specification for Cable Structure (JGJ257-2012) [26] specifies the maximum allowable displacement [σ]=*l*/200= 30mm (*l* is structural span.). The maximum displacement is 9.1mm, which meets the Code's requirements. Judging from the errors between experimental and theoretical values, the errors are within the acceptable range. The main reasons for errors: (1) There is a distinct difference between the final formed shape and design configuration; (2) The strain gauges are slightly drifting in measurements; (3) Measuring instrument will produce some errors.

5.1.2. Under half-span loads

The responses of internal forces and displacement of the structure under half-span loads are shown in Fig. 19.

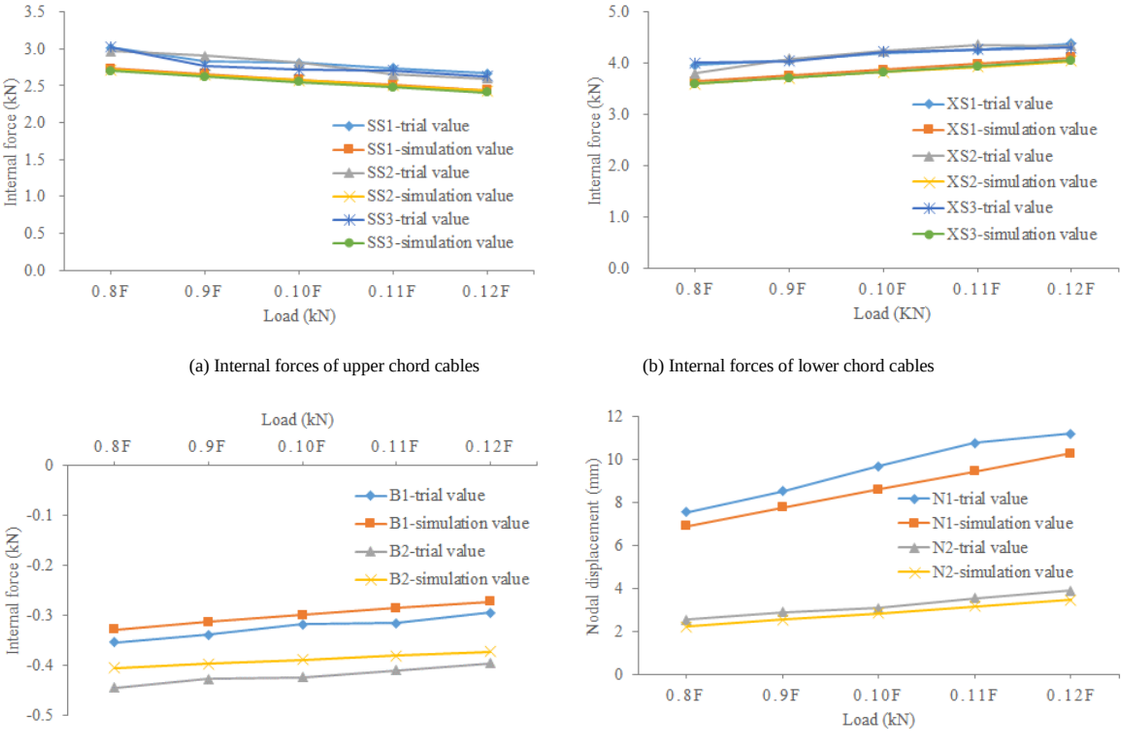

(a) Internal forces of upper chord cables

(b) Internal forces of lower chord cables

(c) Internal forces of struts

(d) Nodal displacement

Fig. 19 Internal forces of cable and strut and nodal displacement under half-span loads

It can be seen from Fig. 19 that the change laws of internal forces of cable and strut and nodal displacement under half-span loads are the same as those under full-span loads. The error range is roughly the same, and the reasons for errors are the same, so it is no longer described again.

5.2. Dynamic experiment

To further verify the correctness of the final formed model, it is necessary to study the dynamic characteristics of SCSWIRC. Meanwhile, SCSWIRC is a new type of CTTS, and its natural vibration characteristics are the basis of wind resistance and earthquake resistance, and no scholars have studied it. In the paper, the final formed model is tested for the dynamic characteristic of the initial prestress state, full-span load state, and half-span load state. The change laws of natural vibration frequency under three conditions are analyzed. The dynamic experiment under loads considers the action of hierarchical load that is the same as **F** in Section 4.1.

In the dynamic experiment, as the structure is symmetrical about the ring direction, three acceleration sensors are installed at different nodes on one side of the structure. The CF0151 acceleration sensors are used, and their positions are shown in Fig. 17. The structural acceleration time curve under external excitation can be obtained through dynamic collection instrument JM3841 shown in Fig. 17. Dynamic signal test and analysis software can calculate structural natural vibration frequency based on the obtained acceleration time curve (JMTEST).

As three CF0151 acceleration sensors on the experimental model, the mean value of three experimental values is seen as the final trial values. Theoretical values can be solved by Block Lanczos Method (LANB) in Ref. [2]. The influence of prestress effect and large deformation on the structure can be considered by setting the prestress stiffening effect and large deformation command in ANSYS finite element software. Based on the above discussions, the first 6-order frequencies of theoretical and experimental values are shown in Table 5-1~5-3.

Table 5-1
First 6 natural frequencies in initial prestress state Unit: HZ

Type	1st order	2nd order	3rd order	4th order	5th order	6th order
S-value	6.809	6.879	7.322	7.541	8.670	8.908
T-value	6.742	6.742	7.296	7.302	8.573	8.574

Description: S-value is simulation value; T-value is trial value, the same as below.

Table 5-2
First 6 natural frequencies in full-span load state Unit: HZ

Load times	Type	1st order	2nd order	3rd order	4th order	5th order	6th order
0.8F	S-value	4.636	4.718	5.364	5.446	6.143	6.263
	T-value	4.419	4.53	5.121	5.124	5.869	5.993
0.9F	S-value	4.371	4.417	5.110	5.314	5.776	5.897
	T-value	4.173	4.213	4.836	4.954	5.541	5.665
1.0F	S-value	4.156	4.221	4.861	4.932	5.412	5.533
	T-value	3.964	3.864	4.593	4.643	5.263	5.385
1.1F	S-value	3.913	3.875	4.494	5.512	5.257	5.372
	T-value	3.784	3.764	4.384	4.422	5.023	5.144
1.2F	S-value	3.825	3.954	4.481	4.521	5.040	5.164
	T-value	3.626	3.752	4.201	4.321	4.813	4.935

Table 5-3
First 6 natural frequencies in half-span load state Unit: HZ

Load times	Type	1st order	2nd order	3rd order	4th order	5th order	6th order
0.8F	S-value	4.402	4.522	4.724	4.865	5.549	5.651
	T-value	4.228	4.320	4.567	4.521	5.370	5.421
0.9F	S-value	4.108	4.230	4.502	4.621	5.196	5.234
	T-value	3.992	4.144	4.313	4.356	5.071	5.112
1.0F	S-value	3.965	4.088	4.203	4.354	5.062	5.134
	T-value	3.792	3.944	4.096	4.126	4.817	4.954
1.1F	S-value	3.819	3.938	4.084	4.132	4.817	4.821
	T-value	3.620	3.762	3.909	4.012	4.597	4.624
1.2F	S-value	3.606	3.724	3.957	4.025	4.590	5.621
	T-value	3.469	3.543	3.746	3.654	4.405	4.251

It can be known from Table 5 that the theoretical values are slightly larger than the experimental values. The main reasons are that the finite element model is a simplified

model. The finite element model's quality is less than that of the experimental model, and its prestress distribution is more uniform than that of the experimental model. From the first 6 frequencies, the 1st order frequency is the same as the 2nd order frequency; the 3rd order frequency is the same as the 4th order frequency; the 5th order frequency is the same as the 6th order frequency, which shows there is a symmetrical axis for the structure. In the initial prestress state, the first 6 order frequencies' theoretical values are in the range of 6.809~8.908HZ, and its experimental values are 6.742~8.574HZ, which shows that structural frequency distribution is dense. Its frequencies gradually increase with the increase of orders. Whether under full-span load state or half-span load, the natural frequency distribution and change laws are the same as those in the initial prestress state. Meanwhile, structural frequencies gradually decrease with the increase of loads, which conforms to the change laws of dynamic characteristics. It can be seen from a characteristic dynamic experiment that experimental values are in agreement with theoretical values indicating that the final formed experiment model is rational and reasonable.

6. Conclusions

In order to solve the difficulty of SCSWIRC's construction forming, a segmented assembly construction forming method without brackets is proposed. Based on the experimental model of SCSWIRC with a diameter of 6m, the segmented assembly construction forming method without brackets is studied by numerical simulation and experimental research.

The results show that experimental values and simulation values are identical. The error range of internal forces of cables and struts is in the range 6.99%~11.58%, and errors of displacement of node 1 and node 2 are 3.27mm and 3.81mm, respectively. The errors are in the acceptable range, which verifies the feasibility of the segmented assembly construction forming method without brackets. Then the static and dynamic experiments are carried out based on the final formed model. Under full-span loads and half-span loads, the error of internal forces of cables and struts is 10% or so; the maximum displacement errors of nodes 1 and 2 are 10.86% and 12.89%, respectively. The errors are in the acceptable range. It can be seen from the dynamic experiment that the experimental values and theoretical values are identical under three conditions. The natural frequency distribution is dense, and natural frequencies increase with the increase of orders. Structural frequencies gradually decrease with the increase of loads, which conforms to the change laws of dynamic characteristics. So, the static and dynamic experiment verifies the correctness and rationality of the final formed model.

The simulation and experimental results verify the feasibility and correctness of the segmented assembly construction forming method without brackets. The proposed new method can solve the difficulty of construction forming.

Acknowledgements

The authors would like to acknowledge the financial support of the National Natural Science Foundation of China (51778017), the National Natural Science Foundation of China (51878014).

References

[1] Liang Xiaotian. Optimization and control research of cable-strut tensile strutctures. Hangzhou: School of Architecture and Engineering, Zhejiang Univesity, 2017.
[2] Xue Suduo，Lu Jian，Li Xiongyan，et al. The influence of grid-jumping arrangement on the static and dynamic performance of annular crossed cable-truss structure. Journal of Jilin University (Engineering and Technology Edition), 2020, 50(5), 1687-1697.
[3] Lu Jian, Xue Suduso, Lu Jian, Li Xiongyan, et al. Key Construction Technology of Annular Crossed Cable-truss Structure. Journal of Tianjin University (Science and Technology), 2021, 54(1), 101-110.
[4] Guo Yanlin, Wang Kun, Tian Guangyu, et al. Research and design of structural form of spoke structure. Journal of Building Structures, 2013, 34(5): 1-10.
[5] Deng Hua, Jiang Q., Kwan A. (2005). Shape finding of incomplete cable-strut assembies containing slack and prestressed elements. Computer Structures, 83,1767-79.
[6] Lu Jian, Xue Suduo, Li Xiongyan, Liu Renjie. Study on membrane roof schemes of annular crossed cable-truss structure. International Journal of Space Structures, 2019, 34(3-4):85-96.
[7] Levy M.P., The Georgia Dome and beyond: Achieving light weight-long span structures, Spatial, lattice and tension structures, proceedings IASS-ASCE international symposium, New York, 1994, pp. 560-562.
[8] Ge J.Q., Zhang A.L., Liu X.G., Zhang G.J., Ye X.B., Wang S., and Liu X.C., "Analysis oftension form-finding and whole loading process simulation of cable dome structure", Journal of Building Structures, 33(4), 1-11, 2012.
[9] Geiger DH. Stefaniuk A, Chen D. The design and construction of two cable domes for the Korean Olympics. Shells, membrane and space frames, proceedings IASS symposium, Osaka, Japan, Vol. 2. p. 265−72.
[10] Geiger D H, Campbell D, Chen D, et al. Design details of an elliptical cable dome and a large span cable dome under construction in the United States//Proceedings,1st Oleg Kerenslry Memorial Conference, London England,1988:14-17.
[11] Levy MP. The Georgia Dome and beyond: Achieving lightweight-longspan structures. Spatial, lattice and tension structures, proceedings IASS-ASCE international symposium, New York. P. 560−2.
[12] Zhang Guojun, Ge Jiaqi, Wang Shu, et al. Design and research on cable dome structural system of the national Fitness Center in Ejin Horo Banner, Inner Mongolia. Journal of building structures, 2012;33(04):12−22.
[13] Sehlaich J, Bergermann R, Goppert K. National Sports ComPlex-Kuala LumPur, Malaysia, Lightweight Roof Structures for the Outdoor Stadium and the Swimming ComPlex[Z], 1997.
[14] Jeon BS, Lee JH. Cable membrane roof structure with oval opening of stadium for 2002 FIFA world Cup in Busan. In: Proceedings of sixth Asian-Pacific conference on shell and spatial structures, vol. 2, Soul, South Korea; 2000. P.1037−42.
[15] Tian Guangyu. Reasearch on Key Technology of Design Theory and Construction Control in Spoke Tension Structures. Tsinghua University, 2012.
[16] Deng Hua, Zhang Minrui, Liu Hongchuang, et al. Numerical analysis of the pretension deviations of novel Crescent-shaped tensile canopy structural system, Engineering Structure,2016;119:24−33.
[17] Liu Renjie, Li Xiongyan, Xue Suduo, Marijke Mollaert, Ye Jihong**.** Numerical and experimental research on annular crossed cable-truss structure under cable rupture. Earthquake Engineering and Engineering Vibration, 2017, 16(3): 557-569.
[18] Shen Shizhao., Xu Chongbao, Zhao Chen. "Suspension structure design", Beijing, China Architecture & Building Press, 17-19, 2006.
[19] Xue Suduo, Lu Jian, Li Xiongyan, Liu Renjie. Improved force iteration method based on rational shape design solving self-stress modes of cable-truss tensile structure, Advanced Steel Construction. 2020,16(2), 170-180.
[20] Zhao Ping, Sun shanxing, Zhou Wensheng. Construtction process inverse simulation analysis of cable dome based on ansys. Industrial Construction, 2013, 43(04), 127-130.
[21] Zhang Ailin, Hu Yang, Liu Xuechun. Numerical simulation analysis and research on the whole construction process of ribbed ring cable structure[A]. Tianjin University, Shanghai University of Jiaotong. Proceeding of the 10th National Symposium on Modern Structural Engineering [C]. Tianjin University, Shanghai University of Jiaotong: Academic Committee of the National Symposium on Modern Structural Engineering, 2010: 6.
[22] Yuan Xingfei, Dong Shilin. Inverse analysis of construction process for cable dome. Journal of building structures, 2001, 22(02), 75-80.
[23] Liu Renjie. Annular Crossed Cable-truss Structures: Numerical and experimental verification. Beijing University of Technology, 2017.
[24] Guo Yanlin., Tian Guagnyu. "Cable structure system, design theory and construction control", Beijing, Science Press, 2014.
[25] Shen Zuyan, Zhang Lixin. Simulation of erection procedures of cable domes based on nonlinear FEM. Journal of Computation Mechanics, 2002, 19(04), 466-471.
[26] Technical Specification for Cable Structure, JGJ257-2012. Beijing: China Architecture & Building Press, 2008.